Volume 17
Number 47
21 December 2025
Pages 9507–9692

Analytical Methods

rsc.li/methods

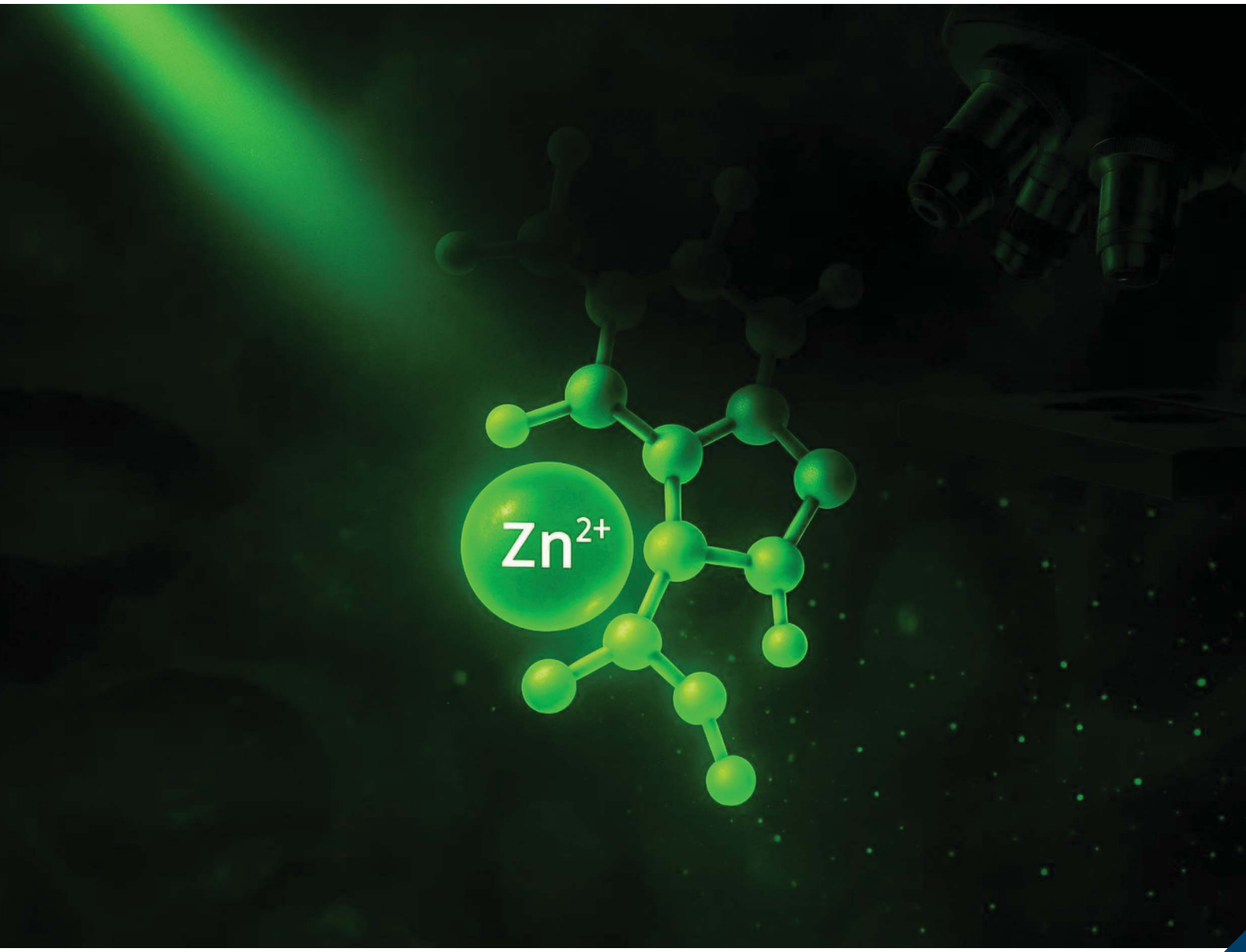

ISSN 1759-9679

ROYAL SOCIETY OF CHEMISTRY

COMMUNICATION
Ozlem Dilek *et al.*
Lighting up zinc: switchable probes for biological imaging

Analytical Methods

ROYAL SOCIETY OF CHEMISTRY

COMMUNICATION

View Article Online
View Journal | View Issue

Cite this: *Anal. Methods*, 2025, **17**, 9530

Received 22nd September 2025
Accepted 7th November 2025

DOI: 10.1039/d5ay01587a

rsc.li/methods

Lighting up zinc: switchable probes for biological imaging

Abisoye O. Fafioye,[a] Beenish Bashir,[b] Andre Clayborne[b] and Ozlem Dilek *[a]

Individual condensation of salicylaldehyde and a variety of different pyridines (equimolar concentration) in polar solution results in a yellowish-orange precipitate (imine-derived product). The study shows that these small-molecule compounds possess turn off and on fluorescence properties upon chelation with Zn^{2+} ions. When reacted with other metal ions, there was no significant increase in the fluorescence intensity of the probes. However, there was multi-fold increase in fluorescence intensity when the probes reacted with Zn^{2+} ions. The probes can be employed as zinc-specific sensors in multiple applications including bioimaging, nanotechnology and environmental sciences.

Zinc is the second most abundant trace element in the human body after iron, constituting approximately 0.004% of total body mass and predominantly existing in the divalent Zn^{2+} state.[1] It is an essential micronutrient involved in numerous physiological processes, including metabolism,[2] neurotransmission,[3] DNA synthesis, apoptosis regulation,[4] immune response[5] and enzymatic function[6]. Due to its central role in these pathways, maintaining optimal zinc homeostasis is critical. Zinc deficiency is associated with developmental delays, impaired immune function, metabolic disorders, and increased susceptibility to certain cancers. Conversely, excessive zinc levels may induce toxicity and are implicated in the progression of several neurodegenerative diseases, including Alzheimer's disease,[7] familial amyotrophic lateral sclerosis,[8] and Parkinson's disease[9,10].

These contrasting outcomes underscore the need for precise, sensitive, and selective detection methods to monitor zinc levels in biological and environmental samples.[11] Among therapeutic approaches, zinc supplementation—particularly using zinc acetate—has demonstrated high bioavailability (~100%) under physiological conditions (pH 7.4) and remains one of the most effective strategies for correcting zinc deficiency.[12,13] Moreover, zinc acetate has been utilized in diagnostic and therapeutic applications, such as injectable formulations for monitoring tumour growth in certain cancers.[14–17] Fluorescence-based detection has emerged as a leading technique for the selective identification and quantification of transition metal ions, notably Zn^{2+}, due to its high sensitivity, real-time monitoring capability, and minimal invasiveness.[18,19] This method has found widespread utility across diverse fields, including cellular biology,[20] nanotechnology,[21–23] and environmental science.[24,25] Fluorescent probes typically comprise three functional components: (i) a fluorophore, which generates a measurable emission upon excitation; (ii) a recognition moiety, which selectively binds the target analyte; and (iii) a linker that connects the fluorophore to the recognition site. Upon interaction with the analyte—such as Zn^{2+}—the recognition event induces a structural or electronic change that activates the fluorophore, leading to a fluorescence response detectable by spectroscopic methods.[26,27] The sensitivity and selectivity of these probes are highly dependent on the electronic configuration of the fluorophore core and its interaction with the target molecule.

Fluorescent probes possessing enhanced spectroscopic properties, high signal-to-noise ratios, and strong target specificity have become indispensable tools in diverse areas including bioimaging,[28,29] environmental monitoring,[30] protein labelling,[31–33] drug development,[34,35] and food safety testing.[36,37] Among these, pyridine-based fluorophores have attracted considerable attention owing to their strong metal-coordination ability, high photostability, and tunable photophysical characteristics, which enable precise modulation of fluorescence intensity and emission wavelength.[38] Continued development of such systems is essential for advancing the understanding of zinc biology and addressing issues related to its dysregulation.

Zinc-sensing fluorescent probes constitute one of the most extensively studied classes of probes for biological imaging due to their operational simplicity, excellent cell permeability, biocompatibility, and negligible interference from competing biological ions.[39,40] Their fluorescence enhancement typically

[a]*Department of Chemistry and Biochemistry, Institute for Advanced Biomedical Research, George Mason University, Manassas, VA, USA*

[b]*Department of Chemistry and Biochemistry, George Mason University, Fairfax, VA, USA. E-mail: odilek@gmu.edu*

arises from zinc coordination, which suppresses photoinduced electron transfer (PET) quenching between the receptor and fluorophore, resulting in a pronounced emissive response.[41] A wide range of zinc-responsive probes based on naphthol, coumarin, rhodamine, and fluorescein scaffolds has been reported; however, these systems are generally of high molecular weight.[42] In contrast, the development of small-molecule fluorophores remains relatively unexplored, despite their potential advantages in terms of synthetic accessibility, sensitivity, and selectivity.

In this work, we report the design and synthesis of a series of small-molecule imine-derived fluorophores (≤320 amu) exhibiting high affinity and selectivity for Zn^{2+} ions. The target compounds were prepared *via* condensation of salicylaldehyde with four pyridine derivatives: 5-aminopyridine-2-carboxylic acid (**1**), 2-amino-3-chloro-5-trifluoromethylpyridine (**2**), 5-amino-2-trifluoromethylpyridine (**3**), and 2-amino-3-hydroxypyridine (**4**) (Scheme 1). Detailed synthetic procedures are provided in the SI.

The structural identity of the synthesized compounds was confirmed by ^{1}H NMR spectroscopy. We found sharp singlet signals in the range of δ 8.66–5.50 ppm, consistent with the formation of imine (–C═N–) functional group. Purity of the probes was confirmed with sharp melting point values and molecular weight on mass spectra (see SI). Following structural confirmation, the UV-Vis absorption and fluorescence responses of the probes to Zn^{2+} ions were evaluated. Schiff bases are well-established as versatile ligands for metal ion coordination due to their electron-rich imine moiety, which facilitates stable complex formation with various metal ions.[43,44] The combination of donor and acceptor groups by a delocalized π-system leads to fluorescence enhancement *via* intramolecular charge transfer (ICT).[45] The synthesized probes demonstrated significant fluorescence enhancement in the presence of Zn^{2+} ions, supporting their potential as metal ion sensors. Solutions of each probe were prepared in methanol at a concentration of 1.0×10^{-3} mM. Zinc acetate stock solution was prepared at the same concentration (1.0×10^{-3} mM) in methanol. Notably, the UV-Vis spectra of probe **1** exhibited no shift in absorption maxima upon Zn^{2+} addition. This suggests minimal perturbation to their ground-state electronic transitions. In contrast, the fluorescence spectrum revealed pronounced changes between probe **1** and its zinc complex. The free probe **1** displayed

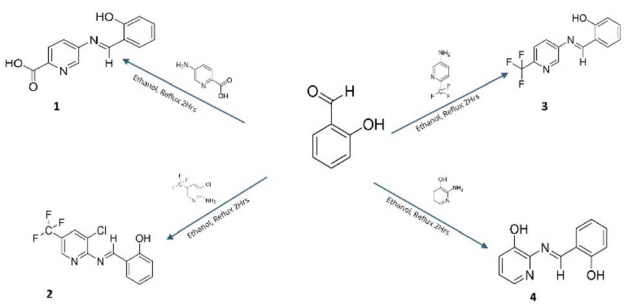

Scheme 1 Schematic diagram of organic synthesis of compounds **1**–**4**.

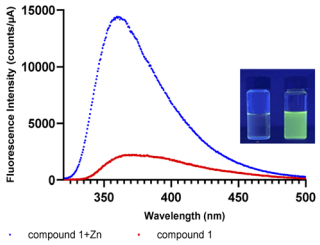

Fig. 1 Emission spectra of free compound **1** (red) and its Zn^{+2} complex (blue) in methanol. Photos of solutions of compound **1** (left) and its zinc complex (right) in methanol under fluorescent light.

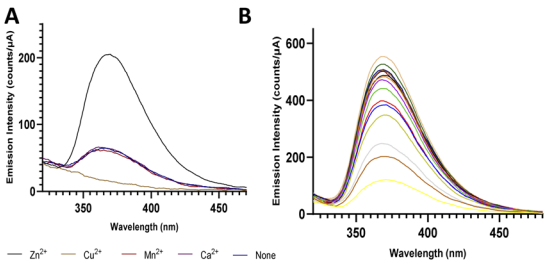

Fig. 2 (A): Emission spectrum of compound **1** complexation with Zn^{2+} when compared with Mn^{2+}, Cu^{2+}, and Ca^{2+}. (B): Fluorescence emission spectra of compound **1** (10 μM) with various amounts of Zn^{2+} (0–1.0 equiv.) in methanol.

moderate emission intensity at a wavelength of about 360 nm, which increased by approximately 4.5-fold upon the addition of Zn^{2+} ions (Fig. 1), indicating a strong fluorescence "turn-on" upon metal binding. The selectivity of probe **1** was examined by reacting the probe with four different metal ions: Zn^{2+}, Mn^{2+}, Cu^{2+}, and Ca^{2+}. Under UV light (short and long wavelengths), only the Zn^{2+}–probe complex displayed bright green fluorescence. The fluorescence intensity of each complex was measured (Fig. 2A). Upon addition of 1.0 equivalent of each metal ion, Zn^{2+} induced a significant enhancement in fluorescence intensity compared to the other ions. In contrast, Mn^{2+}, Cu^{2+}, and Ca^{2+} elicited minimal emission changes (Fig. 2A), indicating high selectivity of probe **1** for Zn^{2+} ions. The observed fluorescence enhancement is attributed to chelation-enhanced fluorescence (CHEF) and inhibition of photoinduced electron transfer (PET) upon Zn^{2+} coordination. Additionally, Zn^{2+} binding likely restricts C═N bond isomerization, further contributing to fluorescence recovery. An intramolecular charge transfer (ICT) process may also be involved in the emission enhancement. A titration experiment (0–1.0 equivalents) was performed with 0.1 equivalent incremental additions of Zn^{2+} to the methanolic solution of probe **1**. The emission intensity increased in a concentration-dependent manner, with a strong peak observed at 366 nm upon excitation at 282 nm (in MeOH). This confirms the quantitative response of the probe to Zn^{2+} ions (Fig. 2B). Probes **2**–**4** also exhibited strong fluorescence enhancement in the presence of Zn^{2+} under UV light. Their absorbance maxima were observed in the blue region at 306 nm, 342 nm, and 358 nm, respectively (Table 1). While probe **2** showed no change in the absorption maxima upon addition of

Table 1 Absorption and fluorescence emission spectra of synthesized compounds (**1–4**) and their zinc acetate ($Zn(OAc)_2$) interaction in methanol

Probe #	$Absorbance_{max}$ (nm)	$Emission_{max}$ (nm)
1	282	360
1+Zn	282	366
2	366	580
2+Zn	368	562
3	342	500
3+Zn	348	520
4	358	520
4+Zn	432	561

Zn^{2+} ions, probe **3** recorded a slight red shift (342–348 nm) while probe **4** showed a significant shift in absorbance maxima from 358 nm to 432 nm after the addition of Zn^{2+} ions.

The development of novel fluorescent probes is essential for the selective detection of target analytes such as metal ions in complex biological samples. Particularly, zinc plays a crucial role in numerous physiological processes, and notably, the prostate contains the highest concentration of zinc in the human body—approximately three to ten times greater than that found in other tissues. However, in prostate cancer (PC), zinc levels are markedly reduced.[46] Several studies have documented up to a six-fold decrease in zinc concentration in cancerous prostate tissue compared to healthy tissue.[47] The current reliance on serum prostate-specific antigen (PSA) as a diagnostic marker for prostate cancer has faced growing criticism due to its limited specificity, which often results in overdiagnosis and overtreatment.[48] In contrast, one of the most consistent biochemical hallmarks of prostate cancer is a significant reduction in intracellular zinc levels.[49,50] This diminished capacity of prostate cells to accumulate and secrete zinc presents a promising avenue for early detection of the disease.

In our preliminary cell-imaging studies, we successfully distinguished healthy prostate cells from malignant ones based on their fluorescence intensity. Upon the addition of probe **1**, tumor cells exhibited markedly lower fluorescence compared to normal prostate cells (Fig. 3), reflecting their reduced intracellular zinc content. To assess the sensitivity of probe **1** to Zn^{2+} ions within cells, prostate cancer cells were incubated with a known concentration of zinc acetate solution (50 μM) and labeled with the probe **1** (10–20 μM). Confocal images of fixed cells—PC-404 (normal) and PC-408 (tumor)—after labeling with probe **1** were captured (Fig. 3). The fluorescence intensity varied between the normal and tumor cells depending on the presence or absence of Zn^{2+}, indicating that the probe effectively responds to intracellular zinc levels.

To gain deeper insight into the photochemical characteristics of the designed pyridine-based fluorophores in the presence of zinc, computational studies were performed using the Gaussian 16 program. The optimized molecular geometries, molecular orbital distributions, and excitation energies of the synthesized probes were calculated to elucidate their electronic structures and photophysical properties (see SI for detailed Computational methods). The optimized structures of amine starting material,

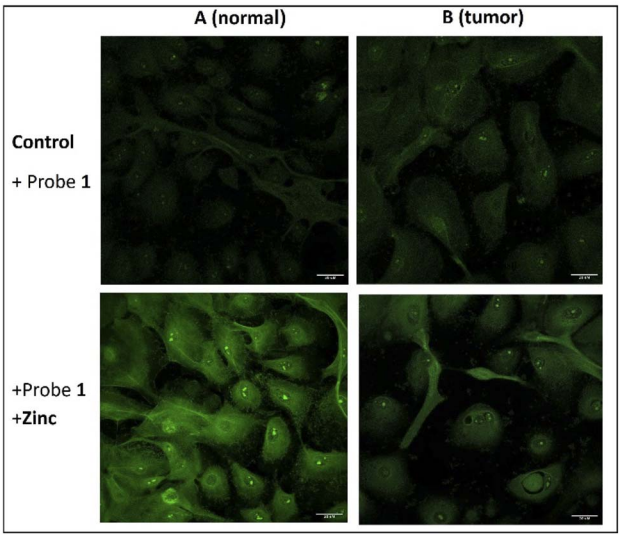

Fig. 3 (A) Labeling normal (404), (B) cancer (408) prostate cells with probe **1** in the presence and absence of zinc.

probe-**1** (the salicylaldehyde imine product), and probe-**1** + Zn are shown in Fig. 4. The frontier molecular orbitals (FMOs), including the highest occupied molecular orbital (HOMO) and the lowest unoccupied molecular orbital (LUMO), were analyzed to gain insights into the electronic properties and electron density distribution patterns. The orbital distributions for amine starting material, probe-**1**, and probe-**1** + Zn are illustrated in Fig. 4. For probe-**1**, the electron density of the HOMO is primarily localized on the aminopyridine ring. Meanwhile, the electron densities of HOMO − 1, LUMO, and LUMO + 1 are delocalized across the entire molecular structure. This delocalization indicates efficient overlap between electron transitions, suggesting facile electron transfer processes. For probe-**1** (salicylaldehyde imine product), the HOMO electron density is also predominantly delocalized on the aminopyridine ring. The HOMO − 1 and LUMO electron densities show significant delocalization on the salicylaldehyde ring, while the LUMO − 1 electron density is distributed similarly to the HOMO, predominantly on the

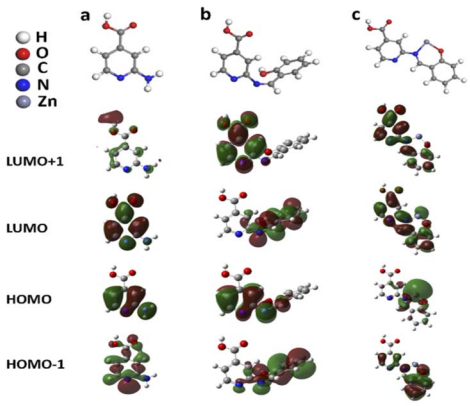

Fig. 4 Optimized molecular structures (top), spatial electronic distributions of HOMO and LUMO energy levels of starting material, probe **1**, and probe **1** + zinc (bottom) respectively.

aminopyridine ring. For probe-**1** + Zn, the introduction of the Zn atom significantly alters the electronic structure. The electron density of the HOMO is primarily localized on the Zn atom, while the HOMO − 1 shows delocalization on the salicylaldehyde ring. In contrast, the LUMO electron density is delocalized across the entire molecular structure, and the LUMO − 1 shows electron density distributed on both the aminopyridine and salicylaldehyde rings. These results highlight significant intramolecular charge transfer (ICT) from the Zn atom (acting as a donor) to the aminopyridine and salicylaldehyde rings. The introduction of Zn into probe-**1** results in noticeable changes in the spatial distribution of the molecular orbitals. These changes alter the position and energy of the HOMO and LUMO levels, significantly affecting the HOMO–LUMO gap. (See SI Document).

The UV-Vis spectrum calculated using TD-DFT revealed absorption maxima at 220 nm, 300 nm, and 362 nm for starting material, probe-**1**, and probe-**1** + Zn, respectively (Fig. S2, SI). A noticeable red shift in the UV-Vis spectra is observed for probe-**1** + Zn compared to probe-**1**. This red shift arises from the redistribution of electron density upon the introduction of Zn, particularly its localization at the metal center. The enhanced ICT from Zn to the aminopyridine and salicylaldehyde rings contributes to the increased fluorescence intensity of probe-**1** + Zn. This property is particularly significant for its application as a zinc-sensing fluorescent probe for biological imaging. The strong fluorescence emission is attributed to the efficient charge transfer facilitated by the Zn atom, making these probes highly suitable for biological imaging applications.

In conclusion, a series of small-molecule imine-based fluorescent probes were synthesized and characterized for selective Zn^{2+} detection. The probes exhibited significant fluorescence enhancement upon Zn^{2+} coordination, driven by chelation-enhanced fluorescence (CHEF) and suppression of photoinduced electron transfer (PET). Among them, probe **1** demonstrated outstanding sensitivity and selectivity toward Zn^{2+}, with minimal interference from other biologically relevant metal ions. Density functional theory (DFT) calculations corroborated the experimental data, showing that Zn^{2+} binding induces intramolecular charge transfer (ICT) and alters the electronic structure to enhance emission intensity (SI). Cell-based imaging further confirmed the capacity of the probe to distinguish between normal and malignant prostate cells based on intracellular Zn^{2+} levels, underscoring its potential application as a zinc-sensitive diagnostic tool. Overall, these findings highlight the promise of small, efficient fluorophores for real-time Zn^{2+} monitoring in biological systems and for early detection of zinc-related pathologies such as prostate cancer or breast cancer.

Conflicts of interest

There are no conflicts to declare.

Data availability

Should any raw data files be needed in another format they are available from the corresponding author upon reasonable request.

The authors declare that the data supporting the findings of this study are available within the paper and its supplementary information (SI). Supplementary information: experimental procedures, supporting data and NMR spectra. See DOI: **https://doi.org/10.1039/d5ay01587a**.

Acknowledgements

We acknowledge the start-up funds provided by the Department of Chemistry and Biochemistry, College of Sciences (COS) at George Mason University. The authors thank Dr Ewa Krawczyk and Dr Moshe Levi from Georgetown University, Medical Centre for providing us the cell lines and technical assistance with cell culture, immunocytochemistry, and image quantification.

Notes and references

1 J. Li, C. Yin and F. Huo, Development of fluorescent zinc chemosensors based on various fluorophores and their applications in zinc recognition, *Dyes Pigm.*, 2016, **131**, 100–133.
2 L. Y. Shen, *et al.*, A Highly Selective Turn-On Fluorescent Probe for the Detection of Zinc, *Molecules*, 2021, **26**(13), 3825.
3 E. L. Que, D. W. Domaille and C. J. Chang, Metals in neurobiology: probing their chemistry and biology with molecular imaging, *Chem. Rev.*, 2008, **108**, 1517–1549.
4 X. Li, *et al.*, A novel 3-Hydroxychromone fluorescence sensor for intracellular Zn2+ and its application in the recognition of prostate cancer cells, *Sens. Actuators, B*, 2017, **245**, 129–136.
5 L. Iovino, *et al.*, Activation of the zinc-sensing receptor GPR39 promotes T-cell reconstitution after hematopoietic cell transplant in mice, *Blood*, 2022, **139**, 3655–3666.
6 M. Hagimori, N. Mizuyama, Y. Tominaga, T. Mukai and H. Saji, A low-molecular-weight fluorescent sensor with Zn2+ dependent bathochromic shift of emission wavelength and its imaging in living cells, *Dyes Pigm.*, 2015, **113**, 205–209.
7 G. Ringgit, S. Siddiquee, S. Saallah and M. T. Mohamad Lal, A sensitive and rapid determination of zinc ion (Zn2+) using electrochemical sensor based on f-MWCNTs/CS/PB/AuE in drinking water, *Sci. Rep.*, 2022, **12**, 1–14.
8 T. Mandal, *et al.*, Terpyridine derivatives as 'turn-on' fluorescence chemosensors for the selective and sensitive detection of Zn2+ ions in solution and in live cells, *Photochem. Photobiol. Sci.*, 2018, **17**, 1068–1074.
9 J. C. Pezzi, *et al.*, Association between DNA methyltransferase gene polymorphism and Parkinson's disease, *Neurosci. Lett.*, 2017, **639**, 146–150.
10 Y. Xu, *et al.*, A simple fluorescent schiff base for sequential detection of Zn2+ and PPi based on imidazo[2,1-b]thiazole, *J. Photochem. Photobiol., A*, 2019, **383**, 112026.
11 L. Fan, J. C. Qin, C. R. Li and Z. Y. Yang, Two similar Schiff-base receptor based quinoline derivate: Highly selective fluorescent probe for Zn(II), *Spectrochim. Acta, Part A*, 2020, **236**, 118347.

12 G. A. Eby, Zinc lozenges as cure for the common cold - A review and hypothesis, *Med. Hypotheses*, 2010, **74**, 482–492.
13 H. Hemilä, J. T. Fitzgerald, E. J. Petrus and A. Prasad, Zinc Acetate Lozenges May Improve the Recovery Rate of Common Cold Patients: An Individual Patient Data Meta-Analysis, *Open Forum Infect. Dis.*, 2017, **4**(2), DOI: **10.1093/ofid/ofx059**.
14 M. R. Shah, *et al.*, Direct intra-tumoral injection of zinc-acetate halts tumor growth in a xenograft model of prostate cancer, *J. Exp. Clin. Cancer Res.*, 2009, **28**, 84.
15 H. J. Zo, J. Y. Song, J. J. Lee, S. Velmathi and J. S. Park, Highly selective response of bipyridyl-incorporated acetyelene dye for zinc acetate, *Talanta*, 2013, **112**, 80–84.
16 P. E. Spiess, Zinc Supplementation and Prostate Cancer, *Prostate Cancer - From Bench to Bedside*, 2011, DOI: **10.5772/1285**.
17 A. S. Prasad, F. W. J. Beck, B. Bao, D. Snell and J. T. Fitzgerald, Duration and severity of symptoms and levels of plasma interleukin-1 receptor antagonist, soluble tumor necrosis factor receptor, and adhesion molecules in patients with common cold treated with zinc acetate, *J. Infect. Dis.*, 2008, **197**, 795–802.
18 J. M. Goldberg, *et al.*, Photoactivatable Sensors for Detecting Mobile Zinc, *J. Am. Chem. Soc.*, 2018, **140**, 2020–2023.
19 K. P. Carter, A. M. Young and A. E. Palmer, Fluorescent Sensors for Measuring Metal Ions in Living Systems, *Chem. Rev.*, 2014, **114**, 4564–4601.
20 M. Z. Alam, S. Ahmad and S. A. Alimuddin & Khan, Synthesis of Fluorescent Pyrazoline Sensors as Versatile Tool for Zinc ion Detection: A Mini-Review, *J. Fluoresc.*, 2025, **35**, 1241–1253.
21 P. Lu and J. Ai, Fluorescence probes and their sensing applications in nanomaterials system, *Talanta*, 2023, **8**, 100248.
22 K. P. Burris and C. N. Stewart, Fluorescent nanoparticles: Sensing pathogens and toxins in foods and crops, *Trends Food Sci. Technol.*, 2012, **28**, 143–152.
23 W. Li, G. S. Kaminski Schierle, B. Lei, Y. Liu and C. F. Kaminski, Fluorescent Nanoparticles for Super-Resolution Imaging, *Chem. Rev.*, 2022, **122**, 12495–12543.
24 S. Morgana, B. Casentini, V. Tirelli, F. Grasso and S. Amalfitano, Fluorescence-based detection: A review of current and emerging techniques to unveil micro/nanoplastics in environmental samples, *TrAC, Trends Anal. Chem.*, 2024, **172**, 117559.
25 T. Ahmad, S. Abdel-Azeim, S. Khan and N. Ullah, Turn-on fluorescent sensors for nanomolar detection of zinc ions: Synthesis, properties and DFT studies, *J. Taiwan Inst. Chem. Eng.*, 2022, **139**, 104507.
26 M. Sohn, D. S. Himmelsbach, F. E. Barton and P. J. Fedorka-Cray, Fluorescence spectroscopy for rapid detection and classification of bacterial pathogens, *Appl. Spectrosc.*, 2009, **63**, 1251–1255.
27 J. Wen, Q. Hua, S. Ding, A. Sun and Y. Xia, Recent Advances in Fluorescent Probes for Zinc Ions Based on Various Response Mechanisms, *Crit. Rev. Anal. Chem.*, 2024, **54**, 3313–3344.
28 (PDF) Colorimetric and fluorescence recognition of zinc acetate for human breast cancer cell (MCF7) imaging : Development of a logic AND GATE, **https://www.researchgate.net/publication/295548426_Colorimetric_and_fluorescence_recognition_of_zinc_acetate_for_human_breast_cancer_cell_MCF7_imaging_Development_of_a_logic_AND_GATE**.
29 Y. An, *et al.*, A novel tetrapeptide fluorescence sensor for early diagnosis of prostate cancer based on imaging Zn2+ in healthy *versus* cancerous cells, *J. Adv. Res.*, 2020, **24**, 363–370.
30 P. R. Sahoo, K. Prakash and S. Kumar, Light controlled receptors for heavy metal ions, *Coord. Chem. Rev.*, 2018, **357**, 18–49.
31 M. Zhu, *et al.*, Advances in fluorescent probes for targeting organelles: Design strategies, applications and perspectives, *Coord. Chem. Rev.*, 2024, **512**, 215893.
32 K. M. Dean and A. E. Palmer, Advances in fluorescence labeling strategies for dynamic cellular imaging, *Nat. Chem. Biol.*, 2014, **10**, 512–523.
33 S. I. Reja, M. Minoshima, Y. Hori and K. Kikuchi, Near-infrared fluorescent probes: a next-generation tool for protein-labeling applications, *Chem. Sci.*, 2020, **12**, 3437–3447.
34 H. Zhu and I. Hamachi, Fluorescence imaging of drug target proteins using chemical probes, *J. Pharm. Anal.*, 2020, **10**, 426–433.
35 N. I. Georgiev, V. V. Bakov, K. K. Anichina and V. B. Bojinov, Fluorescent Probes as a Tool in Diagnostic and Drug Delivery Systems, *Pharmaceuticals*, 2023, **16**(3), 381.
36 A. Rohde, J. A. Hammerl and S. Al Dahouk, Detection of foodborne bacterial zoonoses by fluorescence *in situ* hybridization, *Food Control*, 2016, **69**, 297–305.
37 P. Hildebrandt, *et al.*, Alternative fluorescent labeling strategies for characterizing gram-positive pathogenic bacteria: Flow cytometry supported counting, sorting, and proteome analysis of Staphylococcus aureus retrieved from infected host cells, *Cytometry, Part A*, 2016, **89**, 932–940.
38 A. Shafie and A. A. Ashour, Pyridine-based fluorescent and colorimetric probes: Advances in metal ion detection and cancer cell imaging (2020–2024), *Microchem. J.*, 2025, **213**, 113716.
39 J. Yu, H. Yu, S. Wang and Y. Qi, Progress in research of zinc ion fluorescent probes for biological imaging, *J. Lumin.*, 2024, **266**, 120318.
40 T. Hirano, K. Kikuchi, Y. Urano and T. Nagano, Improvement and Biological Applications of Fluorescent Probes for Zinc, ZnAFs, *J. Am. Chem. Soc.*, 2002, **124**, 6555–6562.
41 M. L. Zastrow, *et al.*, Reaction-Based Probes for Imaging Mobile Zinc in Live Cells and Tissues, *ACS Sens.*, 2015, **1**, 32–39.
42 J. Yang, L. Tang, L. Li, X. Wu and L. Yan, Recent Advances in Organic Small-Molecule Fluorescent Probes for the Detection of Zinc Ions (Zn2+), *J. Fluoresc.*, 2024, **35**(5), 2641–2674.

43 O. Santoro, X. Zhang and C. Redshaw, Synthesis of Biodegradable Polymers: A Review on the Use of Schiff-Base Metal Complexes as Catalysts for the Ring Opening Polymerization (ROP) of Cyclic Esters, *Catalysts*, 2020, **10**, 800.

44 N. Raman, S. Syed Ali Fathima and J. Dhaveethu Raja, Designing, synthesis and spectral characterization of Schiff base transition metal complexes: DNA cleavage and antimicrobial activity studies, *J. Serb. Chem. Soc.*, 2008, **73**, 1063–1071.

45 M. Z. Alam and S. A. Alimuddin & Khan, A Review on Schiff Base as a Versatile Fluorescent Chemo-sensors Tool for Detection of Cu2+ and Fe3+ Metal Ion, *J. Fluoresc.*, 2023, **33**, 1241–1272.

46 M. Bendellaa, *et al.*, Roles of zinc in cancers: From altered metabolism to therapeutic applications, *Int. J. Cancer*, 2024, **154**, 7–20.

47 M. G. Maddalone, *et al.*, Urinary Zinc Loss Identifies Prostate Cancer Patients, *Cancers*, 2022, **14**, 5316.

48 A. Tidd-Johnson, *et al.*, Prostate cancer screening: Continued controversies and novel biomarker advancements, *Curr. Urol.*, 2022, **16**, 197.

49 Y. Zhang, *et al.*, Post-diagnostic Zinc Supplement Use and Prostate Cancer Survival Among Men With Nonmetastatic Prostate Cancer, *J. Urol.*, 2023, **209**, 549–556.

50 S. S. Nejad, *et al.*, The association between zinc and prostate cancer development: A systematic review and meta-analysis, *PLoS One*, 2024, **19**, e0299398.